# CSMC POWER SUPPLY SYSTEM COMPLETES DC 48KA STEADY STATE OUTPUT EXPERIMENT

Hong Lei, Guang Yang

Hefei Institutes of Physical Science, Chinese Academy of Sciences

Hefei, China

Email: redlei@ipp.ac.cn

Li Jiang, Ge Gao, Qiangjian Chen, Linsen Wang, Hua Li, Zhiquan Song, Liuwei Xu Hefei Institutes of Physical Science, Chinese Academy of Sciences

Hefei, China

Corresponding Author: Li Jiang, Ge Gao (jiangli@ipp.ac.cn, gg@ipp.ac.cn)

## **Abstract**

The CRAFT Central Solenoid Model Coil (CSMC) serves as a critical platform for testing the central solenoid system of future Chinese fusion reactors. As a core component of fusion system in fusion reactors, the central solenoid coil plays a pivotal role in confining high-temperature plasma by generating a toroidal magnetic field. The CSMC Power Supply System is essential for delivering operational current to the central solenoid system. Within the CSMC testing framework, this power supply system holds paramount importance, demanding exceptional reliability and stability. It must maintain consistent performance during prolonged operation while mitigating risks such as superconducting magnet power interruptions or equipment damage caused by potential failures. To achieve these objectives, all constituent modules of the power supply system must exhibit superior quality and operational robustness, incorporate redundant architectural designs, and feature comprehensive fault diagnosis mechanisms alongside protective functionalities.

After years of dedicated research efforts, the scientific team has made significant breakthroughs in the development of the CSMC power supply system. During rigorous testing under a 369mH superconducting pure inductive load, the system successfully achieved a steady-state current output of 48 kA. This accomplishment sets a new global record in experimental parameters within this field, establishing world-leading performance benchmarks.

#### 1. INTRODUCTION

The development of high-power magnet power supply systems has long been recognized as a critical challenge in fusion engineering research. Substantial investigative efforts have been dedicated to this cutting-edge domain globally. Publicly available information indicates that the poloidal field power supply system integrated into Japan's JT-60SA tokamak is specifically engineered for precise control over plasma shape, positioning, and stability as FIG. 1. This system distinguishes itself through exceptional precision control capabilities and robust operational reliability, with a rated output current reaching 20kA [1-5]. The Poloidal Field (PF) power supply system of South Korea's KSTAR device adopts a core design philosophy emphasizing high-current delivery capability and precise current regulation as FIG.2. With a rated output current reaching 25kA, this system effectively enables rapid establishment and sustained maintenance of plasma current over extended durations [6-7].

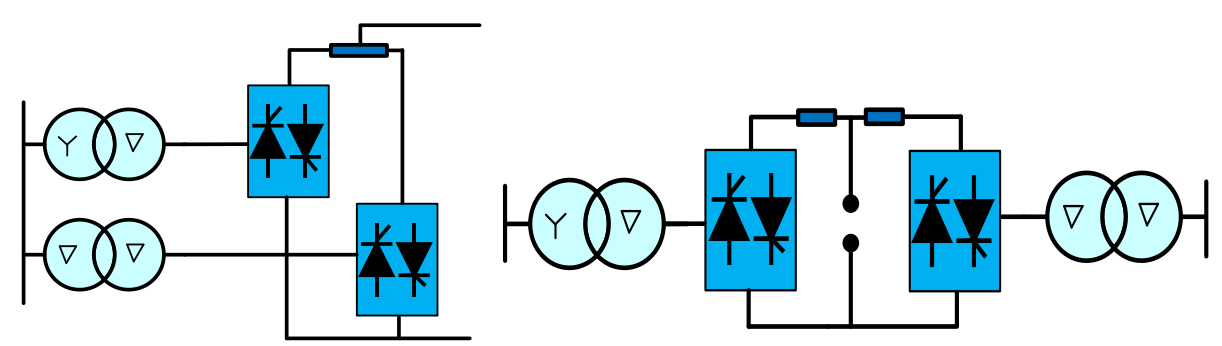


FIG. 1 JT-60SA poloidal field power topology FIG. 2 KSTAR poloidal field power topology Each converter unit within the ITER Poloidal Field Power Supply delivers an output voltage of 1.35 kV and achieves a maximum output current of 55 kA [8-10]. The main topology of the circuit is shown in the FIG.3 below.

FIG. 3. ITER poloidal field power topology

FIG. 4. EAST poloidal field power topology

The EAST Poloidal Field Power Supply comprises twelve independent power units, each employing a thyristor-based three-phase bridge rectifier circuit as FIG. 4. To achieve high-current output capability, each rectifier leg incorporates three parallel-connected thyristors. Regarding topological configuration, ten units (PS1-PS6 and PS9-PS12) utilize an in-phase reverse-parallel connection for their rectifier legs, which ensures high-power output while effectively reducing voltage ripple. In contrast, PS7 and PS8 adopt a non-in-phase reverse-parallel structure. The schematic diagram of the power supply topology is illustrated in the figure [11-12].

The development of high-power superconducting magnet power supply system represents a critical focus in magnetic confinement fusion research, with the CSMC power architecture being a prominent subject of international study. During CSM module testing at ITER, although switch components and power supplies encountered failures at both 10 kA and 15 kA discharge levels (depicted in FIG. 5), the system ultimately achieved a peak test current of 40 kA (illustrated in FIG. 6).

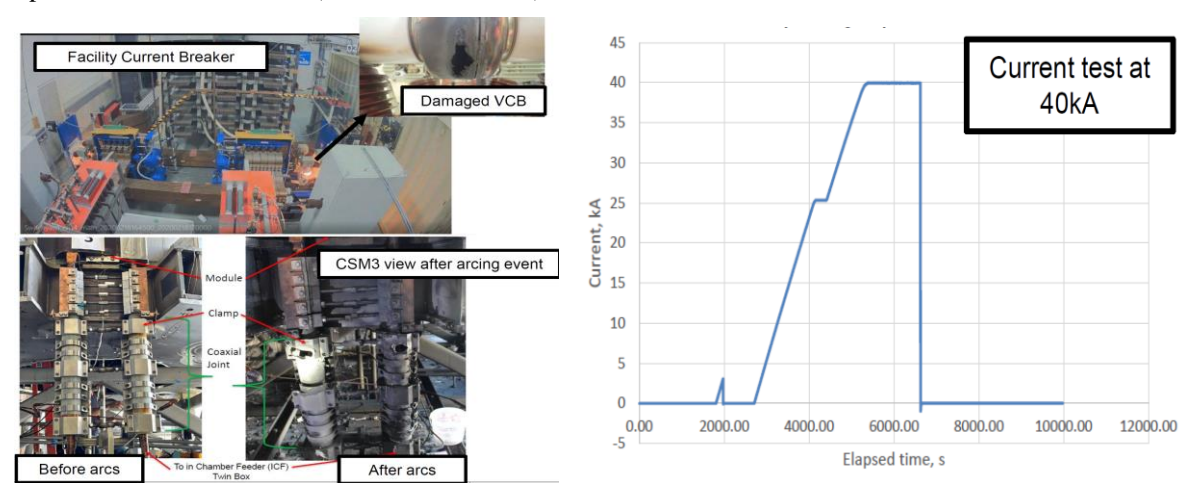


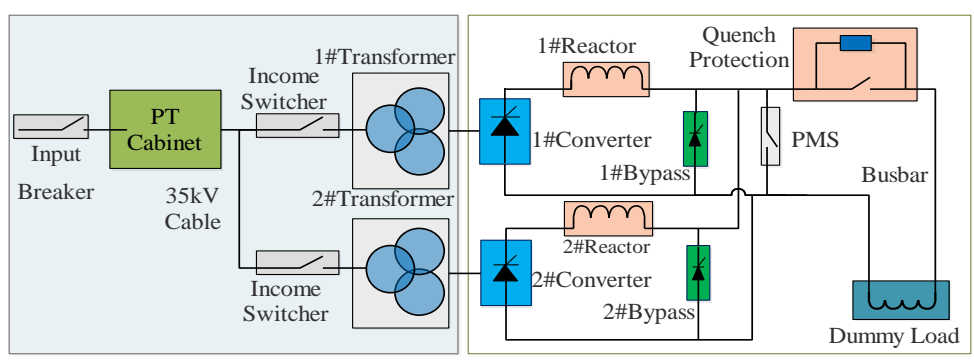
FIG. 5 ITER CSMC Power Supply System

FIG. 6 ITER CSMC Test Current Waveform

# 2. CSMC CONVERTER POWER SUPPLY OPERATING PRINCIPLES

## 2.1. Operating principle of rectifier transformer

The working principle of CSMC rectifier power supply is based on thyristor rectifier technology, and its control mainly considers two aspects. On the one hand, in the parallel mode, multiple rectifier bridge units work in parallel, and each unit is controlled independently to accurately regulate the output current to ensure the balanced distribution of power and system stability. On the other hand, the protection strategy of high power rectifier power supply should be considered. According to the special requirements of superconducting magnet, the power supply system is designed with protection measures such as inverter operation mode and bypass switch, which can effectively release the energy stored in the magnet in case of failure, avoid the damage caused by energy accumulation, and ensure the safety of superconducting magnet and the reliability of power supply system.



AC side electrical equipment

DC and load side electrical equipment

FIG. 7 Topological Diagram of Electrical Equipment

FIG. 7 shows the structure of the CSMC magnet power supply. The topology of the power supply system consists of a step-down transformer, two sets of rectifier transformers, two sets of independent converter units, quench protection system and superconducting load. Each set of converter unit comprises a three-winding rectifier transformer, a three-phase fully-controlled bridge rectifier circuit formed by thyristors, a current-sharing reactor and a bypass switch. The power supply system is supplied by a 110 kV high voltage bus, and the output voltage is reduced to 197 V through a step-down transformer and a rectifier transformer to meet the power supply requirements of the superconducting magnet. In the CSMC magnet power supply, two sets of converters are operated in parallel to realize 12-pulse output, and the primary winding of each rectifier transformer is connected in an extended delta manner to form a required phase difference on the secondary side. The two transformers CU1 and CU2 are connected by the extended delta to achieve a phase shift angle of +22.5° and -7.5° for each transformer, and the phasor diagram of the connection is shown in FIG. 8.

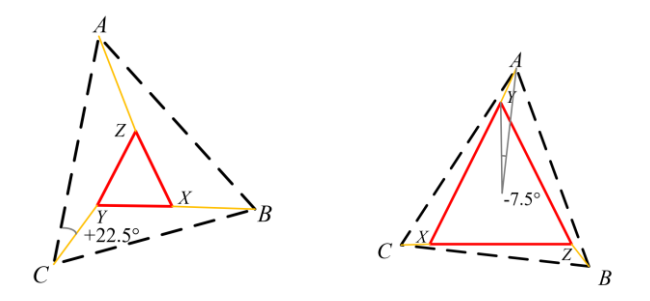


FIG. 8 Phasor diagram of the extended delta connection

# 2.2. Mathematical Model of Rectifier Power Supply

The two groups of converter units in the CSMC magnet power supply have the same topology, and the topology of a single converter unit is shown in the figure, in which the rectifier transformer is equivalent to a three-phase AC power supply as FIG.9. Based on the idealized assumptions, it is assumed that the output voltage of the rectifier transformer has the same amplitude and frequency, and the phase difference between the three phases is  $120^{\circ}$ . In order to simplify the analysis and focus on the basic operating characteristics of the converter, the switching devices are assumed to be ideal switches, and the switching losses and external disturbances are not considered.

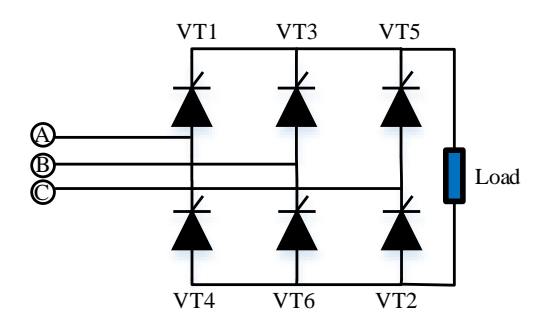


FIG. 9 Topology of a single converter unit

Suppose the output voltage of the rectifier transformer is:

$$\begin{cases} v_a(t) = v_m \sin(\omega t) \\ v_b(t) = v_m \sin(\omega t - \frac{2\pi}{3}) \\ v_c(t) = v_m \sin(\omega t + \frac{2\pi}{3}) \end{cases}$$
 (1)

Where,  $v_m$  present value of output voltage of rectifier transformer.

 $\omega$  frequency of output voltage of rectifier transformer.

The single rectifier unit is a six-pulse rectifier bridge, the output DC voltage pulses six times in a power frequency cycle, and the average value of the output voltage of the rectifier in each pulse when the conduction angle is fixed is:

$$U_0 = \frac{3}{\pi} \int_{\frac{\pi}{3} + \alpha}^{\frac{2\pi}{3} + \alpha} \sqrt{3} v_m \sin(\omega t) d(\omega t) = \frac{2.34}{\sqrt{2}} v_m \cos \alpha$$
 (2)

In the formula,  $\alpha$  conduction angle of bridge arm of rectifier bridge.

In engineering practice, the mathematical model of high-power rectifier power supply when a single rectifier works is as follows:

$$V_0(s) = \frac{K_s}{T_c s + 1} U_{\alpha}(s) - Z_0(s) I_d(s)$$
(3)

In the formula,  $T_s$  represents the delay time of the six-pulse rectifier bridge.

 $K_s$  represents the amplification factor of the six-pulse rectifier bridge.

 $Z_0(s)$  represent that equivalent impedance of the rectifier unit line.

#### 2.3. Single-bridge steady state operation mode

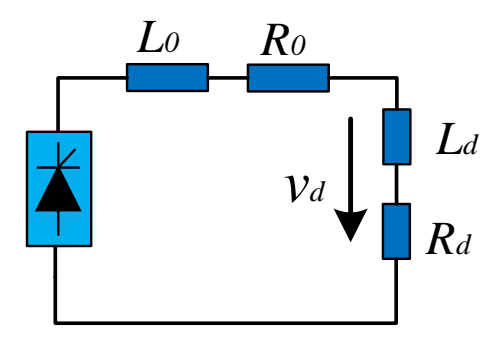


FIG. 10 Equivalent circuit of a single-bridge converter unit

The equivalent circuit of the single-bridge converter unit is shown in FIG.10. The relationship between the load current and voltage in the figure is as follows:

$$\begin{cases} v_d = v_0 - L_0 \frac{di_d}{dt} - R_0 i_d \\ v_d = R_d i_d + L_d \frac{di_d}{dt} \end{cases}$$

$$(4)$$

In the formula,  $v_0$  is the output voltage of the converter.  $L_0$  is the inductance of the current-sharing reactor.  $R_0$  is the equivalent resistance of the line.  $L_d$  is the inductance of the magnet coil.  $R_d$  is the resistance of the magnet coil.  $v_d$  is the voltage at each load end.  $v_d$  is the current at the load end.

Take the Laplace transform of the above equation. For the convenience of analysis, the inductance  $L_0$  of the current-sharing reactor and the equivalent resistance  $R_0$  of the line are combined into the internal impedance of the converter  $Z_0(s) = R_0 + L_0 s$ , and the inductance  $L_d$  of the magnet coil and the resistance  $R_d$  are combined into the load impedance,  $Z_d(s) = R_d + L_d s$ , then:

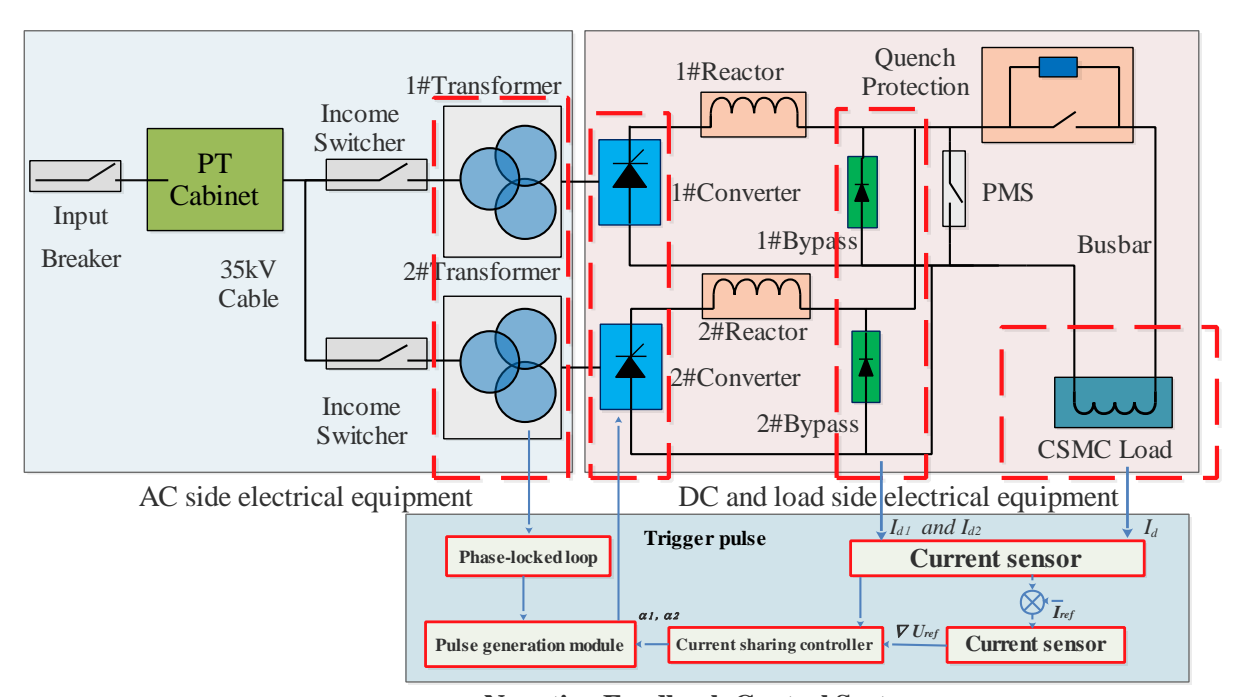
$$\begin{cases} V_d(s) = V_0(s) - Z_0(s)I_d(s) \\ V_d(s) = Z_d(s)I_d(s) \end{cases} \tag{5}$$

The mathematical model of single-branch converter operation can be obtained by combining Formula (2-7) and Formula (6):

$$\begin{cases} V_{d}(s) = V_{0}(s) - Z_{0}(s)I_{d}(s) \\ V_{d}(s) = Z_{d}(s)I_{d}(s) \\ U_{\alpha}(s) = K_{0}[I_{ref}(s) - H_{f}(s)I_{d}(s)] \end{cases} \tag{6}$$

When the output power demand of the power supply system is low, the single-bridge steady-state operation mode is adopted. In this mode, only one of the two rectifier units is put into operation, and the output of the rectifier power supply presents a six-pulse steady-state waveform with a rated output voltage of 250V and a rated output current of 30 kA to meet the requirements of low-power operation conditions.

#### 3. RESEARCH ON CONTROL STRATEGY OF CSMC RECTIFIER POWER SUPPLY



**Negative Feedback Control System** 

FIG.11. Block diagram of negative feedback control system

The load current Id in FIG. 11 is sampled and filtered by a current sensor, and is compared with a preset reference current waveform Iref in real time to calculate a corresponding error signal  $\Delta Id$ , which is input to a negative feedback controller. The negative feedback controller adjusts the output control quantity  $\Delta Uref$  according to the change of  $\Delta Id$ , and cooperates with the current sharing controller to adjust the conduction angle alpha  $\alpha_1,\alpha_2$  of each group of converters. The pulse generation module generates a trigger pulse signal according to the calculated conduction angles  $\alpha_1,\alpha_2$  and a synchronization signal provided by the phase-locked loop, and the trigger pulse signal is used for triggering the thyristor to perform corresponding phase control. The whole control flow of the

system realizes the closed-loop regulation of the output current, ensures that the current stably tracks the set value, and is suitable for loads with high precision and high stability requirements such as superconducting magnets.

According to the mathematical model, the block diagram of the current closed-loop feedback control system for rectifier power supply operation is shown in FIG.12.

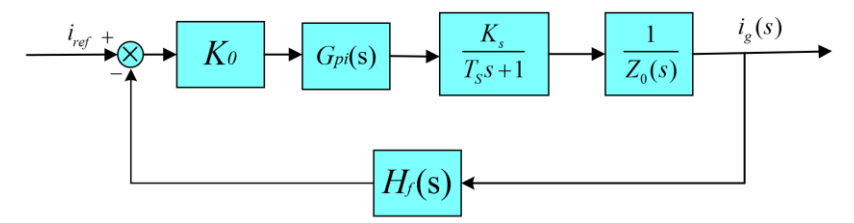


FIG.12. Block diagram of current closed-loop feedback control system

 $H_f(s)$  in FIG.12 is the measurement filtering link, which can be regarded as a first-order low-pass filter  $H_f(s)=1$ . According to the characteristics of the converter,  $T_f$  is 0.0005s,  $K_0$  is the sampling ratio of the current sensor 2.0×  $10^{-4}$ ,  $K_s$  is the amplification factor 93 of the six-pulse rectifier bridge, and  $T_s$  is the delay time 0.00175s of the six-pulse rectifier bridge.

The simulation and tracking results of PI controller are shown in the figure below:

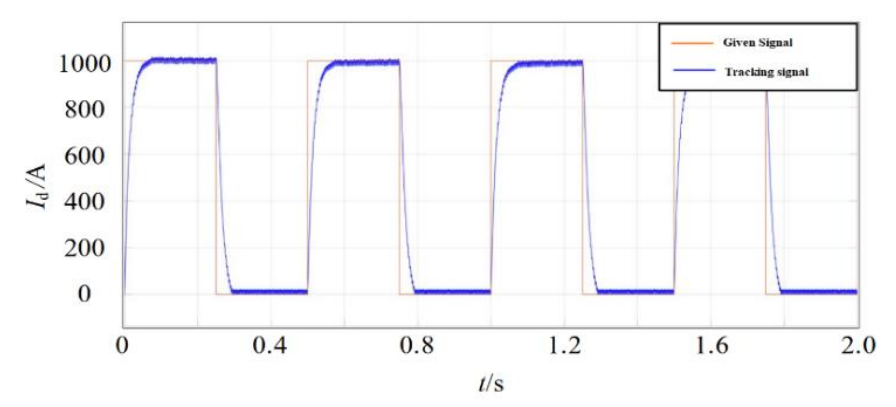


FIG.13 Load current tracking waveform with PI controller

# 4. SIMULATION AND EXPERIMENTAL RESULTS

In order to verify the effectiveness and feasibility of the proposed circuit design scheme and control strategy, a complete simulation model is built on the MATLAB/Simulink platform to simulate the operation characteristics of Tokamak high-power four-quadrant rectifier power supply, and to support the comparison and analysis of control effects under different operating conditions. FIG.14 shows the CSMC power supply simulation experimental model built on the Simulink experimental platform.

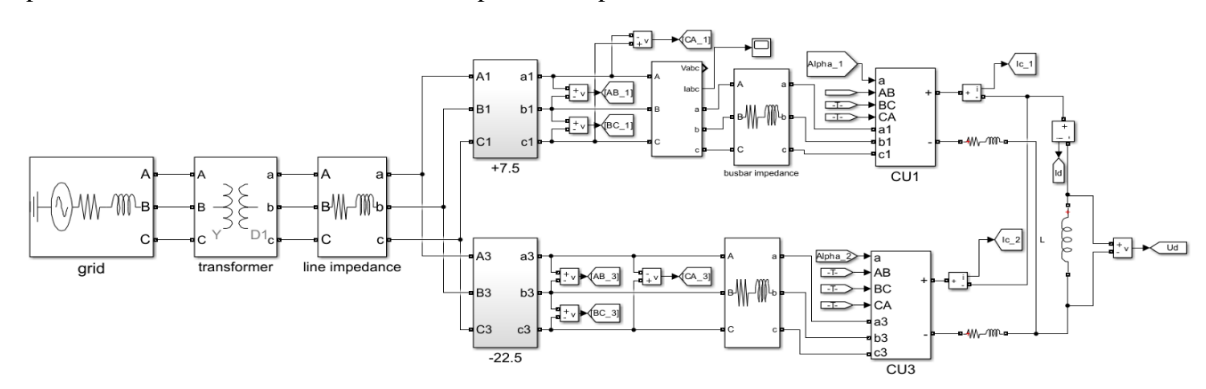


FIG.14 Simulation Model of Converter for CSMC Power System

The main simulation parameters are as follows: the grid voltage part is 110kV three-phase 50Hz AC power supply, the short-circuit capacity is 1.27 GVA, and the ratio of reactance to resistance is 10. The rated capacity of the step-down transformer is 63MVA, the transformation ratio is 110kV/35kV, and the load loss is 232kW. The rated capacity of the rectifier transformer is 8MVA, the transformation ratio is 35kV/197 V, and the load loss is 46kW.

The four rectifier transformers are respectively shifted by  $+22.5^{\circ}$  and  $-7.5^{\circ}$  through extended delta connection. The inductance and internal resistance of the current sharing reactor are  $120\mu H$  and  $120\mu\Omega$ , respectively. The DC side magnet coil load is set to a 4mH inductance.

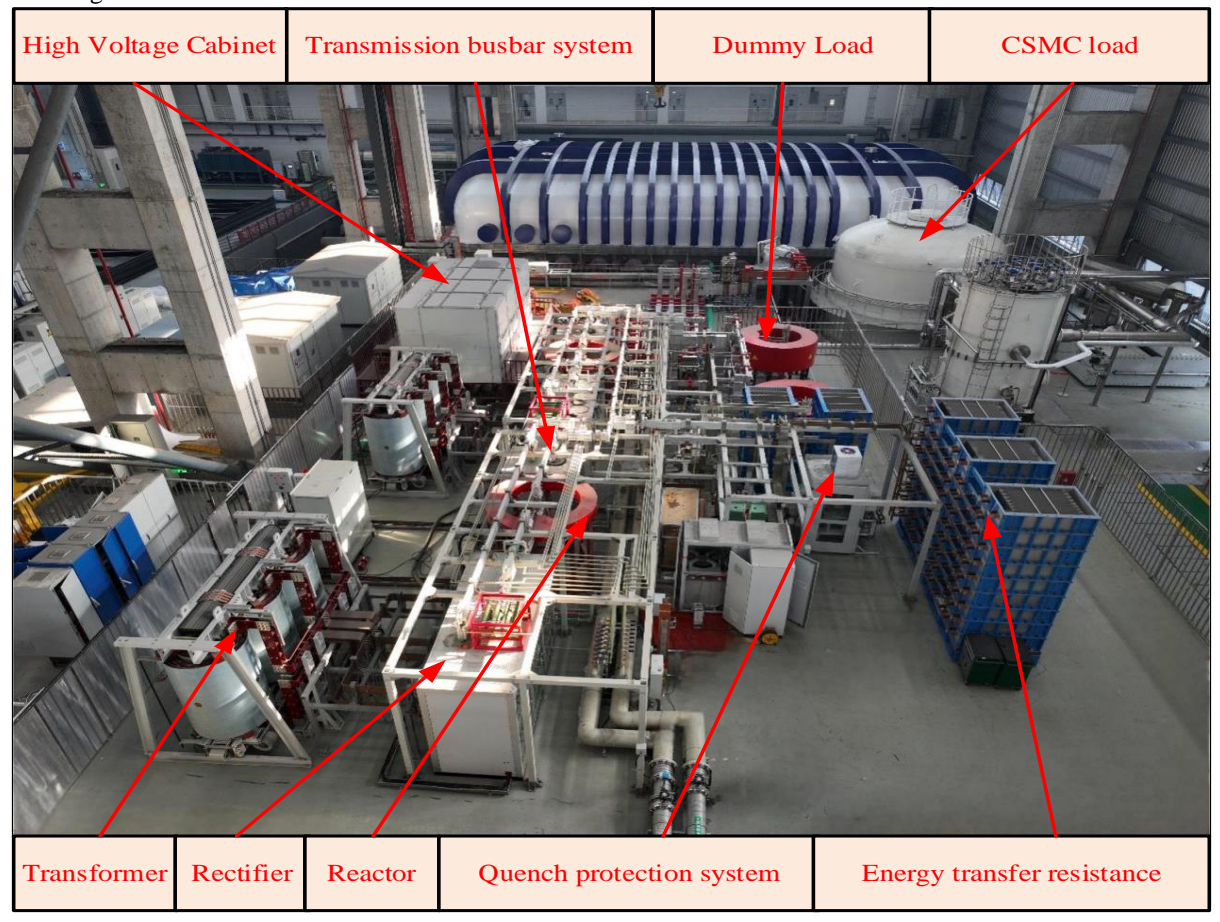
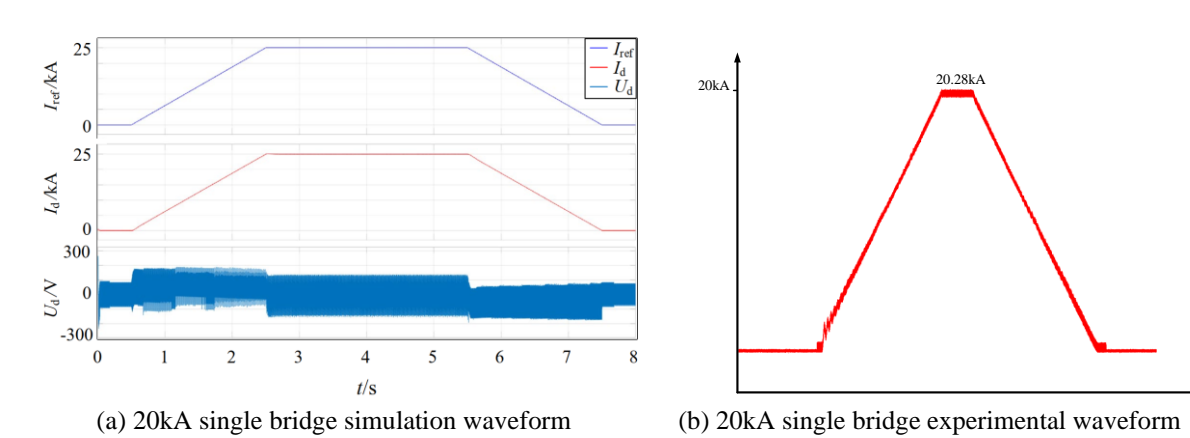
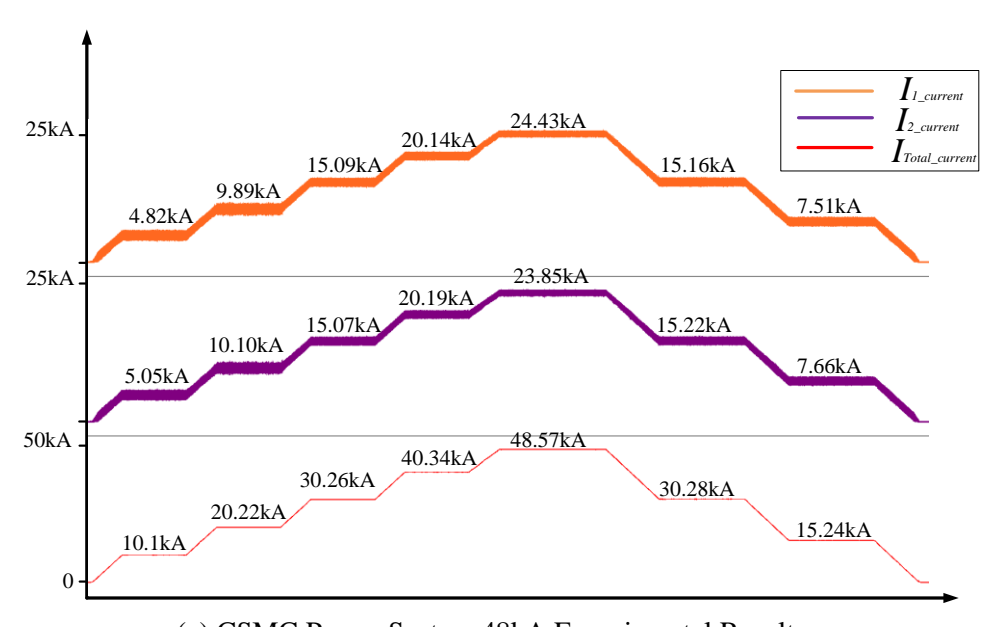


FIG.15 CSMC Power Supply Field Test Device

FIG.14 shows the simulation verification results under the single-branch operation mode: when the reference current command is set as the trapezoidal waveform of 20kA, the load current can track the given waveform command with high accuracy under the condition of 110kV grid voltage input, and there is no significant overshoot or oscillation in the dynamic response process, indicating that the current closed-loop control strategy has good tracking performance and stability.





(c) CSMC Power System 48kA Experimental Results

FIG.15 Simulation and Experimental Results of CSMC Power Supply System

It can be seen from FIG. 15 (c) that the output current of the dual-bridge power supply reaches 48.57kA and the output current of the single-bridge power supply is nearly 24 kA. Due to the current sharing problem of the two power supplies, the current output of the two bridge arms is not even. During the experiment, the temperature of the current lead rises due to the rapid climbing of the current, so the current rise rate is 80 A/s, and it is maintained for a period of time on different current platforms to ensure that the current leader is cooled in time. The experimental data in the FIG.15 is the measured data of the sensor. After calculation, 1.18% of the measurement error is within the allowable error range and output deviation. The whole power-on test verifies the output performance of CSMC power supply system under large inductive load.

## **ACKNOWLEDGEMENTS**

This work was supported by the Comprehensive Research Facility for Fusion Technology Program of China (No. 2018-0000527301001228), Open Fund of Magnetic Confinement Fusion Laboratory of Anhui Province (No. 2024AMF04003) and Natural Science Foundation of Anhui Province (228085ME142).

#### REFERENCES

- [1] Kamada, Y; Di Pietro, E; Hanada, M, et al. Completion of JT-60SA construction and contribution to ITER [J]. Nuclear Fusion, 2022, 62(4): 42002.
- [2] Shimomura Y, Shimizu K, Hirayama T, et al. JT-60 program [J]. Journal of Nuclear Materials, 1984,128:19-25.
- [3] Kikuchi M. The large Tokamak JT-60: a history of the fight to achieve the Japanese fusion research mission I. The European Physical Journal H, 2018,43(4):551-577.
- [4] Lennholm M, Budd T, Felton R. Plasma control at JET. Fusion Engineering& Design, 2000, 48(1/2):37-45.
- [5] Matsukawa M, Shimada K, Yamauchi K, et al. A Conceptual Design Study for the Error Field Correction Coil Power Supply in JT-60SA [J]. Plasma Science and Technology, 2013,15(03): 257-260.
- [6] Kwon M, Oh Y K, Yang HL, et al. Overview of KSTAR initial operation[J]. Nuclear Fusion, 2018, 51(9):94006-94017.
- [7] Shimada K, Baulaigue O, Cara P,et al. Design study of an AC power supply system in JT-60SA[J]. Fusion Engineering and Design, 2011, 86(6):1427-1431.
- [8] Choi J H, Ahn H S, Lee D K, et al. Current control method of thyristor converter for PF superconducting coil in KSTAR. Fusion Engineering and Design, 2012 87(11):1828-1833.
- [9] Perrault D. Status of ITER Safety Issues [J]. Fusion Science and Technology.2019,75(5):1-6.
- [10] Aymar R, Barabaschi P, Shimomura Y, The ITER design [J]. Plasma Physics and Controlled Fusion, 2002, 44(5):519-565.
- [11] Liu L, Zheng W, Zhang X, et al. Design of power and phase feedback control system for ion cyclotron resonance heating in the Experimental Advanced Superconducting Tokamak [J]. Nuclear Engineering and Technology, 2024, 56(1):216-221.
- [12] Song Y, Wu W, Du S. Tokamak engineering mechanics[M]. Berlin: Springer,2014.